Ferroelectric PbTiO3 films grown by pulsed liquid injection MOCVD

Ausrine Bartasyte, R. Bouregba, El Hadj Dogheche, Michel Boudard, G. Poullain, Carmen Jiménez, V. Plausinaitiene, Denis Remiens, Adulfas Abrutis, François Weiss, et al.

▶ **To cite this version:**

Ausrine Bartasyte, R. Bouregba, El Hadj Dogheche, Michel Boudard, G. Poullain, et al.. Ferroelectric PbTiO3 films grown by pulsed liquid injection MOCVD. Surface and Coatings Technology, 2007, 201, pp.9340. 10.1016/j.surfcoat.2007.05.06 . hal-00261249

HAL Id: hal-00261249
https://hal.science/hal-00261249

Submitted on 6 Mar 2008

HAL is a multi-disciplinary open access archive for the deposit and dissemination of scientific research documents, whether they are published or not. The documents may come from teaching and research institutions in France or abroad, or from public or private research centers.

L'archive ouverte pluridisciplinaire **HAL**, est destinée au dépôt et à la diffusion de documents scientifiques de niveau recherche, publiés ou non, émanant des établissements d'enseignement et de recherche français ou étrangers, des laboratoires publics ou privés.

Ferroelectric $PbTiO_3$ films grown by pulsed liquid injection MOCVD

A. Bartasyte[*1,2], R. Bouregba[3], E. Dogheche[4], M. Boudard[5], G. Poullain[3], C. Jimenez[1], V. Plausinaitiene[2], D. Remiens[4], A. Abrutis[2], F. Weiss[1], O. Chaix-Pluchery[1], Z. Saltyte[2]

[1]*Laboratoire des Matériaux et du Génie Physique (CNRS-INP Grenoble), Minatec, 3 parvis Louis Néel, BP 257, 38016 Grenoble Cedex 1, France*

[2]*Vilnius University, Dept. of General and Inorganic Chemistry, Naugarduko 24, LT-03225 Vilnius, Lithuania*

[3]*Laboratoire CRISMAT (CNRS-Université de Caen), Boulevard Maréchal Juin, 14050 Caen Cedex, France*

[4]*Institut d'Electronique, de Microélectronique et de Nanotechnologie, Bat P3, Cité Scientifique, 59655 Villeneuve d'Ascq Cedex, France*

[5]*Science et Ingénierie des Matériaux et Procédés (CNRS-INP Grenoble-UJF), 1130 Rue de la Piscine, BP75, 38402 St. Martin d'Hères Cedex, France*

Abstract

The influence of deposition conditions (pressure, growth rate, solution concentration, etc.) on the growth of ferroelectric $PbTiO_3$ (PTO) films by pulsed liquid injection MOCVD was examined. $Pb(thd)_2$ and $Ti(O^iPr)_2(thd)_2$ (thd = 2,2,6,6-tetramethyl-3,5-heptanedionate) dissolved in toluene were used as precursors. Films were grown on $LaAlO_3$ (001) substrates for deposition process optimisation. $PbTiO_3/La_{1-x}Sr_xMnO_3/LaAlO_3$ heterostructures were elaborated at optimized deposition conditions. The microstructure of the heterostructures was characterized by X-ray Diffraction and by Raman spectroscopy. $Pt/PbTiO_3/La_{1-x}Sr_xMnO_3/LaAlO_3$ structures were used for ferroelectric, dielectric and piezoelectric characterisations of PTO films.

Keywords: MOCVD; $PbTiO_3$ films; ferroelectric and piezoelectric properties.

[*] Corresponding author. E-mail address: Ausrine.Bartasyte@gmail.com

1. Introduction

Ferroelectric $PbTiO_3$ (PTO) and $PbTi_{1-x}Zr_xO_3$ (PZT) thin films are extensively studied since their properties offer a great promise for various applications [1]. High-quality epitaxial ferroelectric films are needed in prospect of new devices; moreover, ferroelectrics can be combined with other functional oxides, such as high temperature superconductors and magnetic oxides. Heterostructures of ferroelectrics with manganites ($La_{1-x}Sr(Ca)_xMnO_3$) exhibiting colossal magnetoresistance are of interest due to the possibility of achieving electric-field-tuned metal-insulator phase transitions, an idea that is being explored for applications based on oxide channel field-effect transistors operating at room temperature [2]. For some applications, epitaxial ferroelectric films must be grown on electrode/substrate. Stresses in such lattice mismatched heterostructures significantly influence both the structural and electrical properties of the films [3]; therefore residual stresses should be evaluated in addition to electrical measurements.

Epitaxial PTO films have been grown by metalorganic chemical vapour deposition (MOCVD) [4, 5], pulsed laser deposition [6] and rf-magnetron sputtering [7]. Among various deposition methods, MOCVD has been recognized as the most promising technique due to simple apparatus, excellent film uniformity, good control of composition and possibility to grow films on large area with high growth rate and good conformal step coverage. Most of PTO film studies are related to structural properties; some papers deal with ferroelectric and dielectric properties [8-12] and a few ones about piezoelectric properties are available [11, 12].

In the present paper, we report on the role of system pressure, solution concentration and injection frequency on the growth rate and composition of $PbTiO_3$ films grown by pulsed liquid injection MOCVD. Further, the $Pt/PbTiO_3/La_{1-x}Sr_xMnO_3/LaAlO_3$ (Pt/PTO/LSMO/LAO) heterostructures were grown and their microstructure, morphology and electrical properties were studied and discussed.

2. Experimental details

Film depositions were carried out in a vertical hot wall pulsed injection MOCVD reactor. This technique is largely described elsewhere [13]. A computer controlled injector repeatedly injects microdroplets of organic solution containing a mixture of metalorganic precursors into a hot evaporation zone. After flash evaporation of microdroplet, resulting vapour is carried out to deposition zone by an $Ar + O_2$ gas flow. Deposition conditions of PTO and LSMO films are summarized in Table 1. More details and discussion on the influence of solution composition,

deposition temperature, oxygen partial pressure and film annealing in different atmospheres on PTO film properties can be found in previous paper [14]. Details about deposition, structural and physical properties of LSMO films are given in Ref. 15.

Film composition was determined by wavelength dispersion spectroscopy (WDS) using Cameca Sx50. The film texture and microstructure were studied by XRD using a SIEMENS D5000 4-circle diffractometer with monochromatic CuK_α radiation (λ=0.15418 nm). An analysis of the microstructure was carried out through standard ω-, χ-, φ-scans. More details concerning this analysis can be found in Ref. 14. Percentage of a-axis oriented domains in the films was calculated by peak integration of (102) reflection in φ-scans measured at different angles, corresponding to a- and c-axis oriented crystallites (i.e. *a*- and *c*-domains, respectively) [14]. The c-parameter of PTO *c*-domains was calculated from the position of three (00*l*) peaks in $\theta/2\theta$ scans. 3D mapping of the reciprocal space was performed with an automatic Nonius Kappa CCD diffractometer (Mo K_α radiation, λ= 0.7071 Å). Film morphology was examined by atomic force microscopy (AFM) using a Digital Instruments Multimode Scanning Probe Microscope, in the taping mode. Thickness of films was determined from cross-section images obtained by SEM Philips XL30.

Raman spectra were collected using Jobin Yvon/Horiba Labram spectrometer equipped with liquid nitrogen cooled CCD detector. Experiments were conducted in the micro-Raman mode at room temperature, in the backscattering geometry. The 514.5 nm line of an Ar^+ laser was focused to a spot size smaller than 1 μm. Spectra from different experiments were calibrated using Si spectra at ambient temperature.

To characterise the ferroelectric properties of PTO films from an electrical point of view, 235 x235 μm^2 square capacitors were designed by UV photolithography using a metallic shadow, and then top contacts were patterned by lift off. Ferroelectric hysteresis loops were observed using a Sawyer-Tower circuit driven at 50 kHz by a sine wave. Capacitance-voltage (C-V) curves and dielectric constants ε_r were determined from small signal capacitance measurements performed at 50 kHz with a HP Agilent LCZ meter. Piezoelectric coefficients d_{33} were measured by laser doppler vibrometry using a Polytec OFV512 as described in Ref. 16.

3. Results

3.1. Effects of film growth rate

As shown in our previous paper [14], Pb fraction in the film grown at higher temperatures (≥600°C) increases until near stoichiometric value and after remains almost stable

with further increase of the Pb content in the solution; thus, Pb excess cannot be reached in the film. In order to observe the maximum Pb/Ti ratio in the film which can be reached by varying the growth rate, lead deficient films were studied. Series of PTO films were deposited at 600 ˚C by varying the total solution concentration (0.02 M, 0.04 M or 0.08 M) and injection frequency (1 Hz or 2 Hz) while the precursors'ratio in solution (Pb/(Pb+Ti)=28.1%) and other deposition conditions were kept constant as given in Table1. The variation of film composition with growth rate is shown in Fig. 1. Pb content in the film increases with increasing growth rate from 4.9 to 10.9 nm/min and saturates when sufficiently high growth rates (>10.9 nm/min) are reached. Deposition with low growth rate results in high Pb desorption from the film. For high growth rates, Pb loss highly decreases and film composition becomes defined mainly by Pb/Ti ratio in solution and precursor's decomposition rates at deposition temperature. In order to obtain Pb/Ti=1 in the films grown with rates >10.9 nm/min, Pb/(Pb+Ti) ratio in the precursor solution should be increased from 28.1% to 31.3% or more. The 0.04 M total concentration and 2 Hz injection frequency were chosen as optimal conditions for further deposition investigation.

3.2. Effects of deposition pressure

In order to test the influence of deposition pressure on PTO film growth, films were grown at 650 ˚C at three different pressures (2, 5 and 10 Torr). The surface of layers deposited at 2 Torr of pressure was completely covered by spherical particles, probably due to precursor decomposition in the reactor volume, thus this pressure was discarded from further investigation. Stoichiometric film was reached using 0.020 M and 0.023 M $Pb(thd)_2$ concentrations (at 0.04 M total concentration of solution) for depositions carried at 5 torr and 10 Torr pressure, respectively. The growth rates of stoichiometric PTO films at 5 Torr and 10 Torr were 20.6 nm/min and 18.8 nm/min, respectively. P. Lu et al. also reported a growth rate decrease of PZT films with increasing pressure [17]. As lower growth rate enhances Pb desorption, higher concentration of lead precursor was needed to obtain stoichiometric PTO at higher pressures.

The results of our present and previous studies on PTO deposition suggest the possibility to control accurately the film growth rate and film composition is important for reproducing stoichiometric PTO films. Therefore, PI MOCVD is a promising method as it offers an easy control of precursor feeding rate, vapour and film composition.

3.3. $PbTiO_3/La_{1-x}Sr_xMnO_3/LaAlO_3$ heterostructures

PTO/LSMO heterostructures consisting of stoichiometric 300 nm thick PTO film and 200 nm LSMO film were grown on LAO at 650 ˚C and 5 Torr pressure using optimal conditions

described above and given in Table 1. The microstructure, surface roughness, residual stresses and electrical properties of the PTO/LSMO/LAO heterostructure are presented and discussed below.

3.3.1. Microstructure and surface roughness

XRD 2D reciprocal space mapping of this heterostructure (Fig. 2a) shows successive epitaxial growth of probably rhombohedral LSMO and tetragonal PTO on LAO substrate along the [00l] direction (referred to pseudo-cubic settings for LSMO). More precise investigations are needed to confirm rhombohedral LSMO structure. Weak reflections in Fig. 2b indicate the presence of PTO crystallites with a-axis oriented almost perpendicular to the substrate plane (*a*-domains). The c-parameter (4.111±0.005 Å) of *c*-domains was reduced compared to the bulk value (4.1532 Å), indicating that PTO film is under tensile stress in-plane. As it is known, the *a*- and *c*-domains are bounded by the (101) twin plane and this results in a tilt of domains by angle from the substrate plane normal depending on the cell tetragonality and domains fraction [18]. The split into four peaks (Fig. 2b) confirms the existence of twinning resulting in tilt of *a*-domains by ~ 2 ˚ angle with respect to the substrate plane. No split was observed for the central reflection in Fig. 2c corresponding to *c*-domains of PTO. The volume fraction of *a*-domains in PTO film was 13.7 %. FWHM of PTO and LSMO rocking curves were 0.64 ˚ and 0.22 ˚ respectively, indicating a good texture quality of the heterostructure. Heterostructure has good in-plane orientation, as FWHM of PTO and LSMO φ-scans were 1.7° and 1° respectively.

Film surface roughness was evaluated by AFM. Higher roughness of PTO films in heterostructure (Ra = 4.3 nm), in comparison with PTO films on LAO (Ra = 0.96 nm), may result from LSMO film roughness (Ra = 2.6 nm). Roughness values are comparable to reported ones for similar heterostructures grown by pulsed laser deposition [19].

3.3.2. Residual stresses

Polarized Raman spectra of PTO/LSMO/LAO heterostructure measured in crossed polarization configuration (VH) confirmed the presence of pure tetragonal PTO phase (Fig. 3), as only *E*(TO) modes are observed [20]. PTO *E*(1TO) soft mode is very pressure sensitive and, as a consequence, its wavenumber shifts as a function of increasing pressure according to the following relation:

$$\omega[E(1TO)] = \omega_0 + (\partial\omega/\partial P)P \qquad (1)$$

where $\omega_0 = 89cm^{-1}$ is the soft mode wavenumber at zero pressure and room temperature, and

$\partial\omega/\partial P = -5.8 cm^{-1} GPa^{-1}$ is the pressure coefficient [21, 22]. The shift value is used to evaluate the residual stress σ in PTO films. PTO E(1TO) mode was observed at 81 cm^{-1} for PTO/LSMO/LAO and at 86.6 cm^{-1} for PTO/LAO. These values, as well as all other E(TO) mode wavenumbers are quite below those observed in single crystal (89 cm^{-1} for E(1TO)). This gives evidence that PTO films on LSMO/LAO and on LAO are under tensile stress in-plane in agreement with XRD results. Corresponding stress values calculated from Eq. 1 are closed to 1.38 and 0.41 GPa in PTO/LSMO/LAO and PTO/LAO, respectively. Despite bigger misfit strain in PTO/LAO system, PTO films on LSMO/LAO were more stressed than PTO/LAO films probably due to distortion induced by rhombohedral structure of LSMO.

3.3.3. Electrical properties

Ferroelectric properties of PTO films on LSMO/LAO were characterized by measuring polarization hysteresis (Fig. 4a). The films displayed hysteresis loops typical of ferroelectric materials for an applied voltage of 6 V. Remanent polarization and average coercive field values were 2.4 $\mu C/cm^2$ and 65 kV/cm, respectively. Quite low remanent polarization values comparing to reported ones [8, 9, 11] can be due to incomplete reversal of the switching domains [11]. However, increasing the applied voltage up to 10 V led to inflating loops typical of non linear lossy dielectrics [23]. The saturation of polarization was not achievable and it was indeed difficult to reach the coercive field due to the leakage currents. The coercive fields are expected to be rather high (>100 kV/cm) due to the strain in the film resulting from epitaxial growth. This fact combined with the leakage current made difficult to observe large polarization in the range of applied voltage. Deposition of stoichiometric PTO films on LSMO/LAO at 10 Torr resulted in films characterized by elliptical hysteresis loops, which is characteristic of excessive leakage currents in the film [24]. Hence, leakage current can be reduced by decreasing lead desorption and then probably the resulting defects.

PTO film deposited at lower pressure displayed capacitance-electric-field curve (Fig. 4b) typical of ferroelectric materials. The dielectric constant of this film reached 325, which is higher than reported values for bulk materials (210 perpendicular to and 120 along polarization direction [25, 26]) and than values published by many authors for PTO films [8-10]. However, Kighelman et al. measured dielectric constant higher than 300 [11]. Higher dielectric constant in our films in comparison with bulk value may be consistent with an increased number of domain walls and with film stresses. Raman spectroscopy results confirmed that PTO films on LSMO/LAO are under tensile stress in the plane parallel to the substrate, despite negative misfit stress. Unlike our

results, Haeni et al. reported enhancement of dielectrical permittivity of $SrTiO_3$ films in case of positive misfit strain but information about stresses was not specified [27]. Dielectric losses (tgα = 0.02) obtained in our films were similar to the reported values.

Using the procedure described in Ref. 16 for an accurate measurement, a small top electrode and a clamped sample have been used to reduce the substrate bending and eliminate the resonant effects. We can illustrate the evolution of the piezoelectric properties of PTO thin films in Fig. 4c. The d_{33} versus E_{dc} loop, measured by laser Doppler vibrometry, was rectangular, with some asymmetry. The piezoelectric coefficient d_{33} measured in PTO films was around 50 pm/V (V_{ac} = 1 V, 48.5 kHz), which is comparable to values reported for PTO films [11] and even for $Pb_{1-x}Ca_xTiO_3$ or PZT films [28, 29]. The asymmetry of piezoelectric and ferroelectric hysteresis and *C-V* loop resulted from the different nature of bottom (LSMO) and top (Pt) electrodes. In fact, the film properties are correlated to the film orientation and control of the film growth results in optimum piezoelectric activity.

4. Conlusions

The growth rate and composition of PTO films were studied as a function of deposition pressure, solution concentration and injection frequency. It was shown, that Pb desorption can be governed by changing film growth rate. Epitaxial PTO/LSMO/LAO films were elaborated at optimized deposition conditions. PTO films in such heterostructure were under tensile stress in-plane; they showed piezoelectric activity and very good dielectric properties, but remanent polarization values were quite low.

References

[1] N. Setter, L. Eng, S. Gevorgian, S. Hong, A. Kingon, H. Kohlstedt, N.Y. Park, G.B. Stephenson, I. Stolitchnov, A.K. Taganstsev, D.V. Taylor, T. Yamada, S. Streiffer, J. Appl. Phys. 100 (2006) 051606.

[2] C.H. Ahn, J.-M. Triscone, J. Mannhart, Nature 424 (2003) 1015.

[3] S.B. Desu, Phys. Status Solidi A Appl. Res. 141 (1994) 119.

[4] C. Schmidt, E.P. Burte, Microeectron. Reliab. 39 (1999) 257.

[5] H. Funakubo, K. Nagashima, K. Shinozaki, N. Mizutami, Thin Solid Films 368 (2000) 261.

[6] Y.K. Kim, S.S. Kim, H. Shin, S. Baik, Appl. Phys. Lett. 84 (25) (2004) 5085.

[7] K. Wasa, Y. Haneda, T. Sato, H. Adachi, K. Setsune, Vacuum 51 (4) (1998) 591.

[8] K. Nishida, T. Sugino, M.Osada, M. Kakihana, T. Katoda, Appl. Surf. Sci. 216 (2003) 312.

[9] D. Bao, X. Yao, N. Wakiya, K. Shinozaki, N. Mizutani, Mater. Sci. Eng. B, Solid State Mater. Adv. Technol. 94 (2002) 269.

[10] H. Huang, X. Yao, X. Wu, M. Wang, L. Zhang, Microelectron. Eng. 66 (2003) 688.

[11] Z. Kighelman, D. Damjanovic, M. Cantoni, N. Setter, J. Appl. Phys. 91 (3) (2002) 1495.

[12] B. Jaber, D. Remiens, E Cattan, P. Tronc, B. Thierry, Sens. Actuators A, Phys. 63 (1997) 91.

[13] J.P. Sénateur, C. Dubourdieu, V. Galindo, F. Weiss, A. Abrutis, Innovative processing of films and nanocrystalline powders, Imperial College Press, London, 2002.

[14] A. Bartasyte, A. Abrutis, C. Jimenez. F. Weiss. O. Chaix-Pluchery, Z. Saltyte, Ferroelectrics 353 (2007) 104.

[15] A. Abrutis, V. Plausinaitiene, V. Kubilius, A. Teiserskis, Z. Saltyte, R. Butkute, J.P. Sénateur, Thin Solid Films 413 (1-2) (2002) 32.

[16] R. Herdier, D. Jenkins, E. Dogheche, D. Remiens, M. Sulc, Rev. Sci. Instrum. 77 (2006) 093905.

[17] P. Lu, H. Li, Y.-M. Wang, S. Sun, B. Tuttle, J. Cryst. Growth 181 (1997) 348.

[18] M. de Keijser, D.M. de Leeuw, P.J. van Veldhoven, A.E.M. de Veirman, D.G. Neerinck, G.J.M. Dormans, Thin Solid Films 368 (2000) 261.

[19] J. Yin, X.S. Gao, Z.G. Liu, Y.X. Zhang, X.Y. Liu, Appl. Surf. Sci. 141 (1999) 21.

[20] M.D. Fontana, H. Idrissi, G.E. Kugel, K. Wojcik, J. Phys., Condens. Matter 3 (1991) 8695.

[21] J.A. Sanjurjo, E. Lopez-Cruz, and G. Burns, Phys. Rev. B 28 (12) (1983) 7260.
[22] F. Cerdeira, W.B. Holzapfel, and D. Bauerle, Phys. Rev. B 11 (3) (1975) 1188.
[23] M.E. Lines, A.M. Glass, Principles and Applications of Ferroelectrics and Related Materials, Oxford University Press, Oxford, 1977, p. 104, reprinted 1996.
[24] R. Bouregba, G. Poullain, Ferroelectrics 274 (2002) 165.
[25] Z. Li, M. Grimsditch, X. Xu, S.K. Chan, Ferroelectrics 141 (1993) 313.
[26] V.G. Gavrilyachenko, E.G. Fesenko, Sov. Phys. Crystallogr. 16 (1971) 549.
[27] J.H. Haeni, P. Irvin, W. Chang, R. Uecker, P. Reiche, Y.L. Li, S. Choudhury, W. Tian, M.E. Hawley, B. Craigo, A.K. Tagantsev, X.Q. Pan, S.K. Streiffer, L.Q. Chen, S.W. Kirchoefer, J. Levy, D.G. Schlom, Nature 430 (2004) 758.
[28] A. Kholkin, A. Seifert, A. Setter, Appl. Phys. Lett. 76 (2000) 1615.
[29] S. Hiboux, P. Muralt, T. Maeder, J. Mater. Res. 14 (1999) 4307.

Figure captions

Fig. 1: PTO/LAO film composition evolution as a function of growth rate.

Fig. 2: 2D sections of the reciprocal space of a PTO/LSMO/LAO structure: (a) $k = 0$ plane; (b) $l = -3.9$ plane; (c) $l = -3.7$ plane.

Fig. 3: Polarized Raman spectra of PTO/LAO, PTO/LSMO/LAO and LSMO/LAO films measured in VH polarization configuration.

Fig. 4: Electrical characterizations of PTO/LSMO/LAO films: (a) polarization hysteresis loop ; (b) capacitance-electric-field curve ; (c) piezoelectric displacement versus E_{dc} loop.

Table 1: Deposition conditions for $PbTiO_3$ and $La_{1-x}Sr_xMnO_3$ layers by PI MOCVD

	$PbTiO_3$	$La_{1-x}Sr_xMnO_3$
Substrates	$LaAlO_3$ (001) in a pseudo-cubic setting	$LaAlO_3$ (001) in a pseudo-cubic setting
Substrate temperature (°C)	600 or 650	800
Evaporation temperature (°C)	280	310
Transport gas	Ar +O_2	Ar + O_2
Total gas flow rate (l/h)	60	95
Oxygen fraction (%)	37.7	35
Total pressure (Torr)	2-10	5
Precursors*	$Pb(thd)_2$,$Ti(thd)_2(O^iPr)_2$	$La(thd)_3$, $Mn(thd)_3$, $Sr(thd)_2$
Solvent	toluene	monoglyme
Solution concentration (total) (mol/l)	0.02-0.08	0.049; with proportion of the precursors: $Sr(thd)_2$:$La(thd)_3$:$Mn(thd)_3$ = 1:1.5:1.58
Injection frequency (Hz)	1or 2	2
Thickness (nm)	200-340	200

* All precursors were synthesized in Vilnius University.

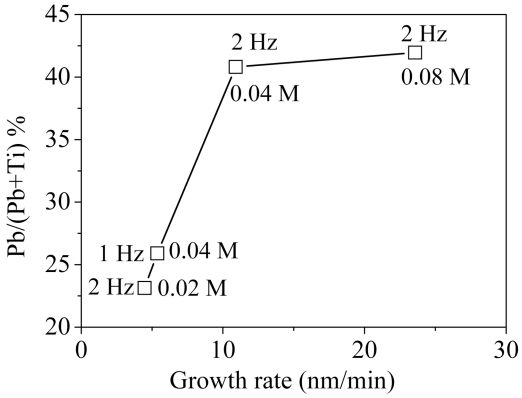

Fig. 1

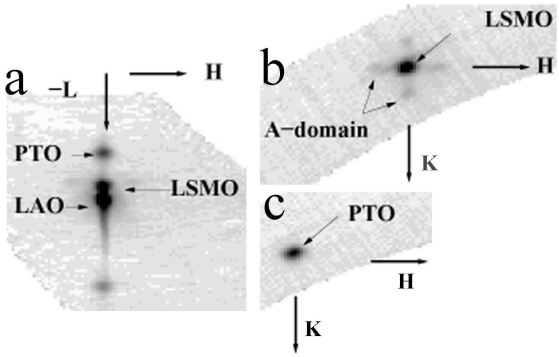

Fig. 2

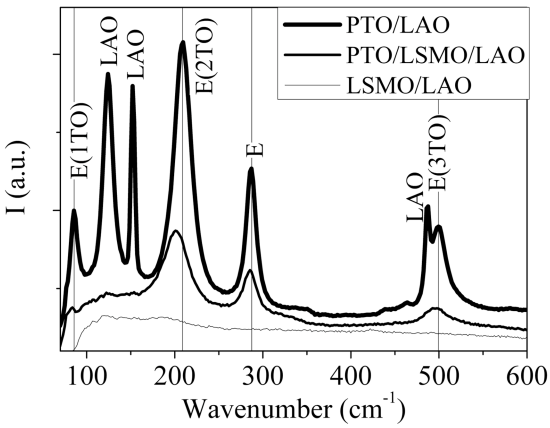

Fig. 3

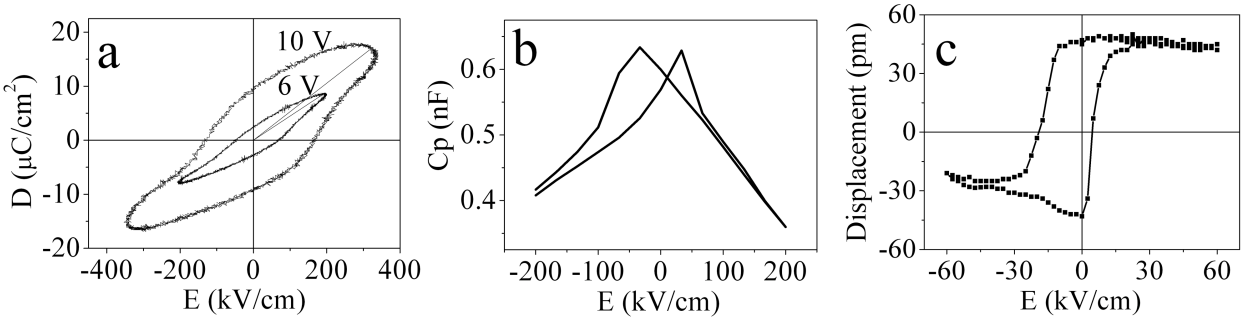

Fig. 4